

# Optical, dielectric and opto-electrical study of Se–Te–Ge glassy thin films

H. E. ATYIA<sup>a</sup>, S. S. FOUAD<sup>a</sup>, PANKAJ SHARMA<sup>b,\*</sup>, A. S. FARID<sup>a</sup>, N. A. HEGAB<sup>a</sup>

<sup>a</sup>*Physics Department, Faculty of Education, Ain Shams University, Cairo, Egypt*

<sup>b</sup>*Department of Physics & Materials Science, Jaypee University of Information Technology, Waknaghat, Solan, H.P. (173234) India*

Addition of germanium to the Se–Te alloy causes change in the optical, dielectric and henceforth the opto-electrical and physical properties of Se–Te–Ge alloys.  $Se_{80}Te_{15}Ge_5$ ,  $Se_{80}Te_{13}Ge_7$  and  $Se_{80}Te_{10}Ge_{10}$  amorphous thin films have been prepared from corresponding glasses on the microscopic glass slides via vacuum resistive heating. The optical band gap of these thin films has been resolved from the transmission spectra and found to increase from 1.54 eV to 1.62 eV. Dielectric constant ( $\epsilon$ ) has been determined from the values of refractive index ( $n$ ), extinction coefficient ( $k$ ) calculated using Swanepoel approach and found to decrease with the addition of Ge content. Some theoretical parameters have also been calculated. The changes in optical parameters with composition of the thin films have been interpreted on the basis of the theoretical parameters *i.e.* lone-pair electrons, coordination number, glass forming ability, deviation of stoichiometry and electronegativity. The variation of the greater part of the specified parameters is due to the change in covalent characters of the films under investigation.

(Received December 14, 2017; accepted June 7, 2018)

**Keywords:** Thin films, Chalcogenides, Optical properties, Dielectric properties

## 1. Introduction

Amorphous materials have attracted much attention after the discovery of chalcogenide glasses, which are utilized as a part of various optoelectronics applications in different areas. Chalcogenide glasses are disordered non-crystalline materials which are generally strongly bonded materials than oxide glasses [1-3]. The lack of long range arrangements and variation in chemical composition allows the modification in the optical properties of chalcogenide glasses. Physical properties of chalcogenides such as high non-linearity refractive index make them ideal for active devices. Se–Te alloys are promising glasses and are widely used in technological and commercial purposes such as, holographic solar cell [4], infrared and recently in re-writable optical data recording [5,6]. Ge–Se system is widely studied system [7-10]. The noncrystalline Se–Te–Ge glassy alloys are useful as a good photovoltaic material, mixing the Se–Te alloy with Ge, enlarges the glass forming region and also create integrative disorder in the system and effects the structural, optical and physical properties [11-15].

In the present work, we have researched some of the experimental and theoretical results based on the optical, dielectric and optoelectric properties of  $Se_{80}Te_{20-x}Ge_x$  ( $x = 5, 7$  and  $10$ ) thin films. The optical energy gap both experimentally and theoretically has been estimated, and the dielectric constants and some other related parameters has also been calculated and discussed. The experimental results of Se–Te–Ge glasses has been interpreted in terms of different theoretical parameters.

## 2. Experimental details

Three compositions of  $Se_{80}Te_{15}Ge_5$ ,  $Se_{80}Te_{13}Ge_7$  and  $Se_{80}Te_{10}Ge_{10}$  have been formed by the melt quenching method given in details in previous work [16]. The structure identification for the three compositions under study was affirmed by X-ray diffraction (XRD) and electron dispersive X-ray spectrum (EDX) analysis discussed elsewhere [17]. Thin films of the glasses were deposited under vacuum of  $10^{-5}$  Torr, by thermal evaporation technique. The details have been given elsewhere [16,17]. A double beam spectrophotometer (UV-310PC Shimadzu) has been used for obtaining the transmission spectra of the prepared films in 500 nm to 2500 nm wavelength range. All the above mentioned measurements have been performed at room temperature.

## 3. Results and discussion

### 3.1. Transmission spectra and optical parameters

The optical transmission data has been utilized for calculating the optical parameters *i.e.* refractive index ( $n$ ) and extinction coefficient ( $k$ ). Fig. 1 presents the transmission spectra of  $Se_{80}Te_{15}Ge_5$ ,  $Se_{80}Te_{13}Ge_7$  and  $Se_{80}Te_{10}Ge_{10}$  thin films with nearly the same thickness  $\approx 450$  nm. The envelope method proposed by Swanepoel [18,19] has been employed to evaluate the values of  $n$ ,  $k$  and the thickness of the measured films for different compositions. The details of the method used for the

determination of the optical parameters may be seen elsewhere [2,18-19].

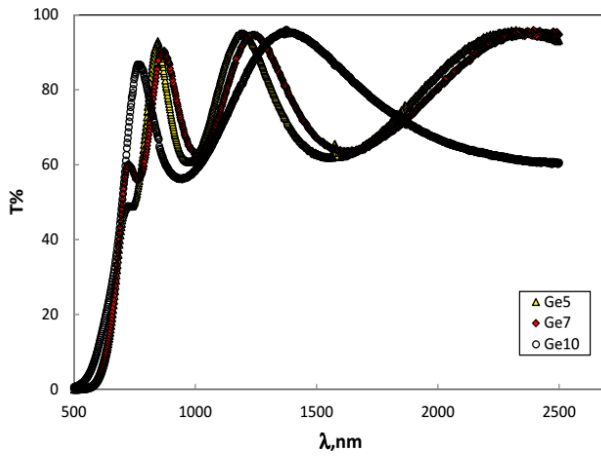


Fig. 1. Transmission spectra of  $\text{Se}_{80}\text{Te}_{15}\text{Ge}_5$ ,  $\text{Se}_{80}\text{Te}_{15}\text{Ge}_7$  and  $\text{Se}_{80}\text{Te}_{10}\text{Ge}_{10}$  films with nearly the same thickness

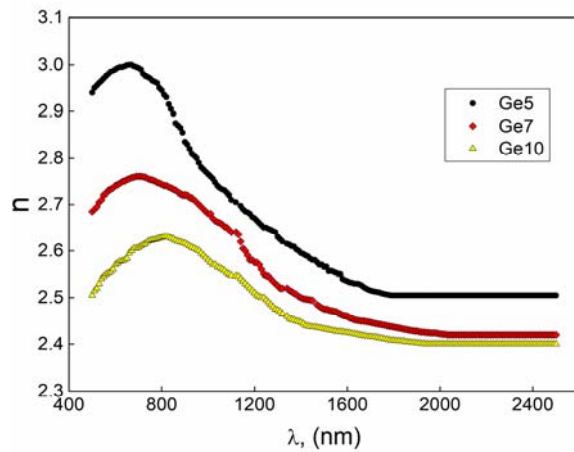


Fig. 2. Spectral behavior of refractive index ( $n$ ) for  $\text{Se}_{80}\text{Te}_{20-x}\text{Ge}_x$  ( $x = 5, 7$  and  $10$ ) film compositions

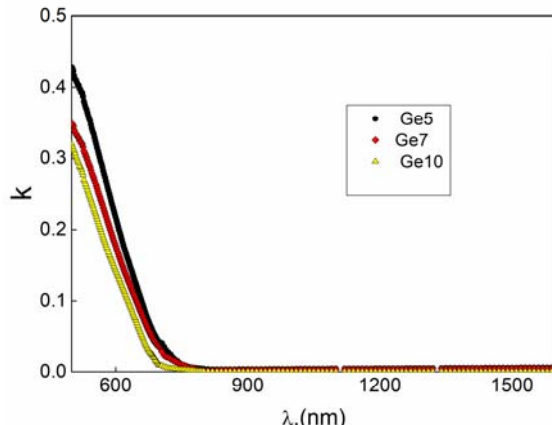


Fig. 3. Spectral behavior of extinction coefficient ( $k$ ) for  $\text{Se}_{80}\text{Te}_{20-x}\text{Ge}_x$  ( $x = 5, 7$  and  $10$ ) film compositions

Figs. 2 and 3 reveal the spectral dependence of  $n$  and  $k$  with wavelength ( $\lambda$ ). As seen,  $n$  exhibits an anomalous dispersion for  $\lambda < 820$  nm while for  $\lambda > 820$  nm,  $n$  shows a standard dispersion. The values of both  $n$  and  $k$  have been found to fall with the increase of  $\lambda$  as well as  $\text{Ge}$  content. The decrease in  $k$  with  $\lambda$  indicates that the portion of light lost is attributable to the scattering that causes a decrease in absorbance. This decrease in the values of  $n$  with  $\text{Ge}$  content may also be in analogy with the atomic polarizability of sample elements. Considering the Lorentz-Lorenz relation the atomic polarizability will decrease with the decrease of atomic radius. So there is a decrease in refractive index values on account of the atomic radius of  $\text{Ge}$  (122 pm) which is less than the atomic radius of  $\text{Te}$  (135 pm). Our results have been well supported by earlier studies [11,20-22].

### 3.2. Analysis of the dispersion parameters

The dispersion parameters play a significant part in understanding the features of the optical materials. Employing the single effective oscillatory model suggested by Wemple and Didomenico (WDD) [23,24], one can be competent to examine the dispersion energy parameters. WDD [23,24] found that both crystalline and amorphous materials can be defined by the following equation;  $(n^2 - 1) = (E_o E_d) / (E_o^2 - (h\nu)^2)$ , where  $h\nu$  is the photon energy,  $E_o$  is the average energy gap or oscillator energy and  $E_d$  is the oscillator strength or the dispersion energy.

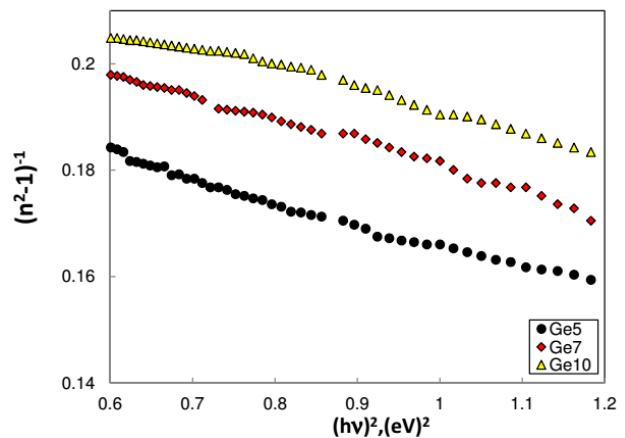


Fig. 4. Variation of  $(n^2 - 1)^{-1}$  vs.  $(h\nu)^2$  for  $\text{Se}_{80}\text{Te}_{20-x}\text{Ge}_x$  ( $x = 5, 7$  and  $10$ ) film compositions

Fig. 4 represents the plot of  $(n^2 - 1)^{-1}$  against  $(h\nu)^2$  for the three compositions under study. The values of the oscillator parameters ( $E_o$  and  $E_d$ ) can be directly determined from the slopes and intercepts of characteristics given in Fig. 4. For  $h\nu \rightarrow 0$ , WDD equation can be rewritten for static refractive index ( $n_o$ ) as

$n_o = (1 + (E_d / E_o))^{0.5}$ . The high frequency dielectric constant  $\varepsilon_\infty$  has been determined from the relation;  $\varepsilon_\infty = n_o^2$ . The estimated values of  $E_o$ ,  $E_d$ ,  $n_o$ , and  $\varepsilon_\infty$  are listed in Table 1.

Table 1. Some optical parameters of  $Se_{80}Te_{20-x}Ge_x$  ( $x = 5, 7$  and  $10$ ) thin film compositions

| Parameter                        | Value                 |                       |                         |
|----------------------------------|-----------------------|-----------------------|-------------------------|
|                                  | $Se_{80}Te_{15}Ge_5$  | $Se_{80}Te_{13}Ge_7$  | $Se_{80}Te_{10}Ge_{10}$ |
| $E_o$ , (eV)                     | 2.28                  | 2.58                  | 2.79                    |
| $E_d$ , (eV)                     | 10.56                 | 11.74                 | 12.38                   |
| $\varepsilon_L$                  | 6.32                  | 5.98                  | 5.87                    |
| $\varepsilon_\infty$             | 6.32                  | 6.02                  | 5.93                    |
| $n_o$                            | 2.37                  | 2.35                  | 2.33                    |
| $N/m^*$ ,<br>( $m^{-3}kg^{-1}$ ) | $2.45 \times 10^{55}$ | $2.34 \times 10^{55}$ | $1.59 \times 10^{55}$   |
| $E_g^{opt}$ ,(eV)                | 1.54                  | 1.58                  | 1.62                    |
| $E_U$ ,(eV)                      | 0.118                 | 0.105                 | 0.068                   |
| $E_g^{WD}$ ,(eV)                 | 1.52                  | 1.72                  | 1.86                    |
| $E_g^{th}$ ,(eV)                 | 1.705                 | 1.724                 | 1.74                    |

It can be seen that the obtained values of the dispersion energy parameters  $E_o$  and  $E_d$  increase with an increase in the *Ge* proportion at the expense of *Te* content. The lattice dielectric constant ( $\varepsilon_L$ ) dependence of the  $\lambda$  and  $n$  has been given by the relation [4];  $n^2 = \varepsilon_L - (Ne^2/4\pi^2m^*\varepsilon_o c^2)\lambda^2$ , where  $N$  is the carrier concentration,  $m^*$  is the effective mass,  $c$  is the velocity of light,  $e$  is the electron charge and  $\varepsilon_o$  is the free space dielectric constant. The dependence of  $n^2$  on  $\lambda^2$  has been found to be linear at higher wavelength (Fig. 5).

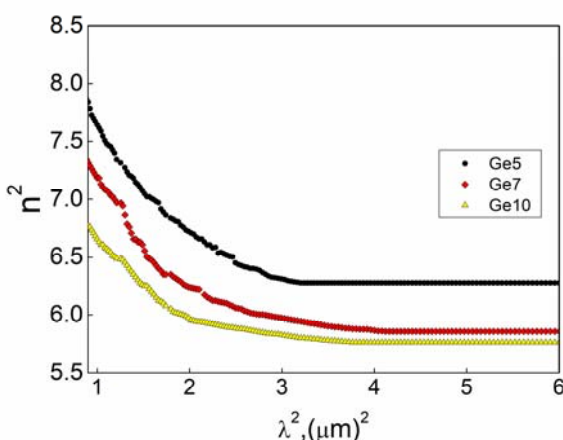


Fig. 5. Variation of  $n^2$  vs.  $\lambda^2$  for  $Se_{80}Te_{20-x}Ge_x$  ( $x = 5, 7$  and  $10$ ) film compositions

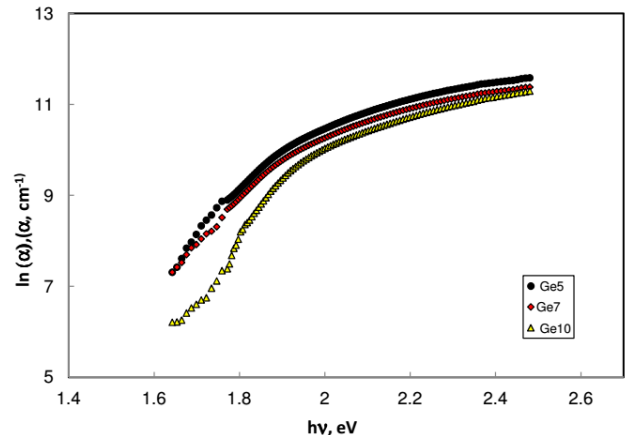


Fig. 6. Photon energy dependence of  $\ln \alpha$  for  $Se_{80}Te_{20-x}Ge_x$  ( $x = 5, 7$  and  $10$ ) film compositions

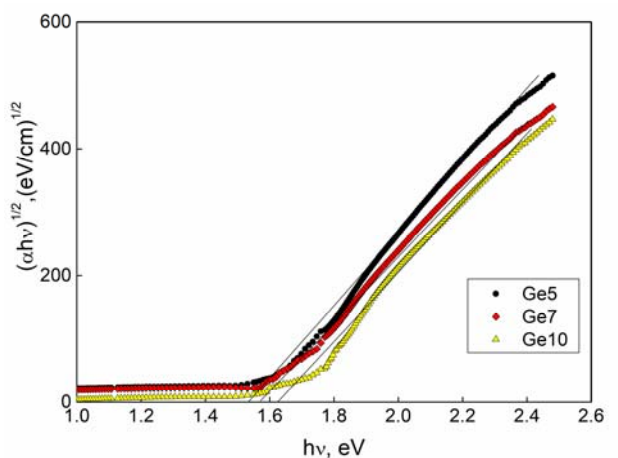


Fig. 7. Photon energy dependence of  $(\alpha h\nu)^{1/2}$  for  $Se_{80}Te_{20-x}Ge_x$  ( $x = 5, 7$  and  $10$ ) film compositions

The values of  $\varepsilon_L$  and the ratio of carrier concentration to effective mass have been determined by deriving  $\lambda^2 = 0$  and from the slopes of these plots respectively. The values of  $\varepsilon_L$  and  $(N/m^*)$  are given in Table 1. As seen from Table 1 the composition dependent values of  $\varepsilon_L$  and  $\varepsilon_\infty$  are in good agreement with each other. The spectral distribution of the absorption coefficient ( $\alpha$ ),  $\alpha = 4\pi k/\lambda$ , has been took to examine the sort of the existing optical transitions (Fig. 6). The absorption edge has been examined to show the effect of replacing *Te* with *Ge* for optical band gap values and the type of optical band gap transitions, according to Tauc's relation [25];  $\alpha h\nu = B(h\nu - E_g^{opt})^r$ , where  $B$  is a constant and is called band tail parameter,  $E_g^{opt}$  is the optical band gap and  $r$  is the power factor which identifies the type of optical transitions in the gap. The nature of these thin films has been noticed to be indirect, after fitting different values of  $r$ . Plotting  $(\alpha h\nu)^{1/2}$  versus photon energy and extrapolating the linear part for  $h\nu$  approaching zero (Fig. 7) for all thin films under study. The point where the extrapolated line meets the photon energy axis

provides the values of the indirect optical gap  $E_g^{opt}$  for  $Se_{80}Te_{20-x}Ge_x$  ( $x = 5, 7$  and  $10$ ) thin films. The  $E_g^{opt}$  values are given in Table 1. The values of optical band gap have been found to enhance with the increase of  $Ge$  proportion. Similar results have been given in literature [26]. Many authors [13,27,28] confirmed the decrease of  $E_g^{opt}$  with increasing  $Te$  content in  $GeSeTe$  ternary system and vice versa. In most amorphous materials the absorption coefficient dependence on photon energy is known as Urbach empirical relation [29,30],  $\ln\alpha = \ln\alpha_0 + (h\nu/E_U)$ , where  $\alpha_0$  is constant and  $E_U$  is the band tail width of the localized states in the optical gap. The behavior of  $\ln\alpha$  against  $(h\nu)$  for the three compositions under study have been given in figure 6. The Urbach band tail width ( $E_U$ ) values estimated from the slopes of the straight lines and have been reported in Tables 1. It has been observed that  $E_U$  values decrease with increasing the  $Ge$  content.  $E_U$  corresponds to the transition between tail and the band state and is considered as a measure of the randomness in the glass structure. Enhancing the  $Ge$  content in  $Se$ — $Te$ — $Ge$  thin films results in the blue shifting of the absorption edge of  $E_g^{opt}$ , while the decrease of  $E_U$  is attributed to the lessen in the disordered atoms and defects in the structural bonding. The value of  $E_g^{opt}$  has also been deduced from the empirical WDD dispersion relation;  $E_o = (3/2)E_g^{WD}$  [24]. The values of  $E_g^{WD}$  obtained from this relations have been given in Table 1 for the three compositions under study. The band gap has been calculated theoretically according to Shimakawa's relation [31];

$$E_g^h(Se - Te - Ge) = AE_g(Se) + BE_g(Te) + CE_g(Ge),$$

where A, B and C are the volume fraction of  $Se$ ,  $Te$  and  $Ge$  respectively, and  $E_g(Se)$ ,  $E_g(Te)$  and  $E_g(Ge)$  are the energy gap values of  $Se$  (1.95 eV),  $Te$  (0.65 eV) and  $Ge$  (0.95 eV) respectively. The values of  $E_g^h$  are presented in Table 1. Comparing the values of  $E_g^{opt}$  from the Tauc's with  $E_g^{WD}$  and  $E_g^h$  values, we can easily observe that the variation of the optical gap follow the same trend with increasing  $Ge$  % and decreasing  $Te$  content. Our results are in harmony with other ones reported in literature [32,33].

The optical conductivity ( $\sigma$ ) for thin films depends strongly on the optical band gap and other related parameters such as the absorption coefficient and refractive index.  $\sigma$  can be calculated by using the relation;  $\sigma = \alpha nc/4\pi$  [34], where  $c$  is the speed of light. Fig. 8 shows the dependence of optical conductivity upon photon energy for the investigated thin film compositions. As seen the optical conductivity enhances with raising the photon energy, this is due to the electron's excitation by photon energy.

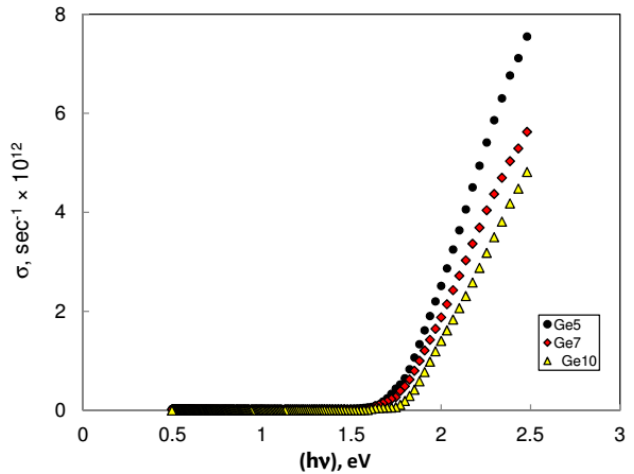


Fig. 8. Variation of optical conductivity with the photon energy for  $Se_{80}Te_{20-x}Ge_x$  ( $x = 5, 7$  and  $10$ ) film compositions

### 3.3. Theoretical interpretation of the experimental optical data

The lone-pair electrons ( $L$ ) play an important role in chalcogenide glasses comprising a large amount of group VI elements ( $Se$  and/or  $Te$ ). Lone pair electrons constitute the top of the valence band while the anti bonding bond makes the bottom of the conduction band [1]. Lone-pair electrons are equal to  $L = V - N_c$ , where  $V$  is valance electrons and  $N_c$  is the average coordination number. The average coordination number characterizes the electronic properties of semiconductor material and it represents the bonding character in the nearest-neighbor regions.  $N_c$  has been calculated using the standard method [35];  $N_c = (aN_{Se} + bN_{Te} + cN_{Ge})/(a + b + c)$ , where  $N_{Se} = 2$ ,  $N_{Te} = 3$ ,  $N_{Ge} = 4$ , while  $a$ ,  $b$  and  $c$  are the atomic ratios of  $Se$ ,  $Te$  and  $Ge$  respectively. The results are listed in Table 2. It has been seen from Table 2, that  $N_c$  increases while  $V$  and  $L$  lessen with the raise of  $Ge$  content. The decrease in  $L$  might be due to the interaction between  $Ge$  ions and the lone-pair electrons of  $Se$  atoms [36-37]. According to Hruby [38] the glass forming ability is;  $K_{ga} = (T_c - T_g)/(T_m - T_c)$ , where  $T_g$  is the glass transition temperature,  $T_c$  is the crystallization temperature and  $T_m$  is the melting temperature. The  $T_g$ ,  $T_c$  and  $T_m$  for the three studied compositions have been taken from the DTA curves reported elsewhere [17] for the samples under study and the calculated  $K_{ga}$  values are listed in Table 2. As seen from Table 2, the values of  $L$  and  $K_{ga}$  are having the same trend i.e. decrease with increasing  $Ge$  content. This result is induced by the interaction of  $Ge$  ions and the lone-pair electron of bridging  $Se$  in the glass network [36,37]. This interaction has influence on the glass formation ability. According to Liang [36] criterion, for computing the ability of any system to retain its vitreous state in case of ternary system the number of lone-pair electrons must be larger than one. The results shown in Table 2 support the above criterion reasonably well.

Table 2. Theoretical parameters of  $Se_{80}Te_{20-x}Ge_x$  ( $x = 5, 7$  and  $10$ ) thin film compositions

| Parameter | Value                |                      |                         |
|-----------|----------------------|----------------------|-------------------------|
|           | $Se_{80}Te_{15}Ge_5$ | $Se_{80}Te_{13}Ge_7$ | $Se_{80}Te_{10}Ge_{10}$ |
| $N_c$     | 2.25                 | 2.27                 | 2.30                    |
| $L$       | 3.65                 | 3.59                 | 3.50                    |
| $V$       | 5.90                 | 5.86                 | 5.80                    |
| $K_{ga}$  | 0.458                | 0.390                | 0.369                   |
| $R$       | 10.25                | 7.11                 | 4.75                    |
| $\chi$    | 2.442                | 2.450                | 2.451                   |

The parameter  $R$  determines the ratio of covalent bonding prospects to the non-chalcogen possibilities and has been termed as the deviation from stoichiometry. For  $Se_{80}Te_{20-x}Ge_x$  ( $x = 5, 7$  and  $10$ ) thin films  $R$  is defined as [39];  $R = (a N_{Se} + b N_{Te})/c N_{Ge}$ , where  $a, b$  and  $c$  are the atomic fraction, and  $N_{Te}$ ,  $N_{Se}$  and  $N_{Ge}$  are the coordination number of  $Te$ ,  $Se$  and  $Ge$  respectively. The glassy alloy is considered to be chalcogen rich for  $R > 1$  and is believed to be chalcogen poor if the value of  $R < 1$ . It can be seen that, the calculated values of  $R$  have been found to be  $> 1$  (Table 2) and show a decrease with the addition of  $Ge$  content. This confirms that our system turning towards less chalcogen with the increase of  $Ge$  content in the system under study. The results have been supported by previously calculated parameters *i.e.*  $N_c$ ,  $L$ ,  $K_{ga}$ . Electronegativity ( $\chi$ ) of the glassy alloy is the geometric mean of electronegativity of its components. The electronegativity values of the atoms involved in our system according to ref. [40] are 2.55 for  $Se$ , 2.10 for  $Te$  and 2.01 for  $Ge$ . The calculated values of  $\chi$  have been listed in Table 2.

Table 3. Percentage Ionicity and covalent character of the expected combination for  $Se_{80}Te_{20-x}Ge_x$  ( $x = 5, 7$  and  $10$ ) thin film compositions

| Bonds   | Ionicity | Covalent character |
|---------|----------|--------------------|
| $Se-Te$ | 4.94     | 95.06              |
| $Se-Ge$ | 7.04     | 92.96              |
| $Te-Ge$ | 0.21     | 99.79              |

According to Philips- Thorpe bond constraint theory [41], the coordination number has some ionic character. Ionicity of a bond has been calculated by using Pauling relation [42];  $Ionic\ character\ \% = 1 - e^{-0.25(\chi_A - \chi_B)^2}$ , where  $(\chi_A - \chi_B)$  is the difference in the electronegativity of atoms involved in bond formation. A direct connection has been found [41] between the strength of bond and the glass formation. For large values of bond strength the glass forming tendency is high and vice versa. Chalcogenide glasses have been made from elements such as  $Se$ ,  $Te$ , and

$Ge$  having predominant covalent bonds. The degree of covalence in the bond of the glassy alloys under investigation has been calculated according to [42] as  $Covalent\ character\ \% = e^{-0.25(\chi_A - \chi_B)^2}$ . The calculated iconicity and covalent character of the expected combination for the compositions under study are given in Table 3. Glass forming ability ( $k_g$ ) of the elements is high if they have more than 90% of covalent character. The presence of  $Ge$  replacing  $Te$  leads the composition towards more ionic in character. In conclusion all the above mentioned parameters have been affected by  $Ge$  addition.

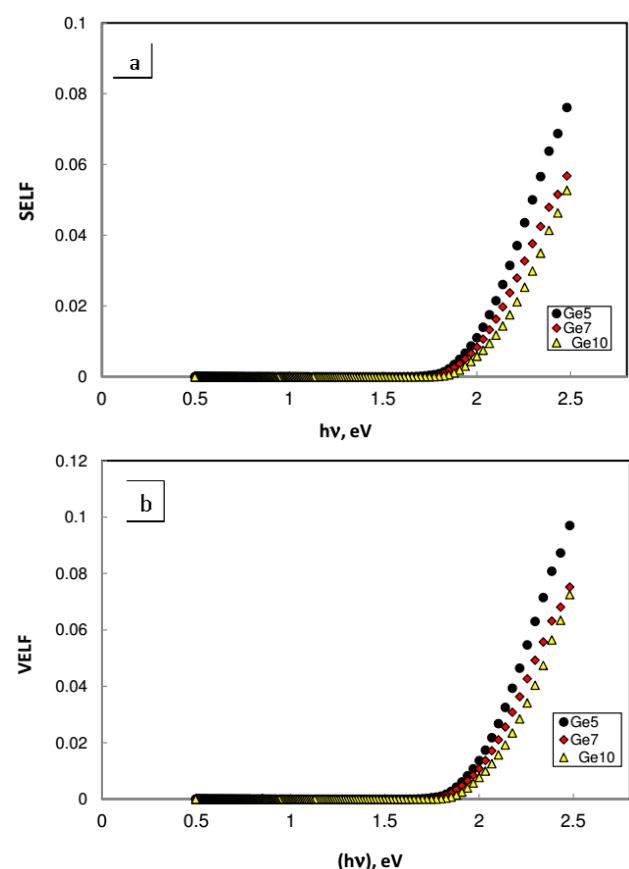


Fig. 9. Plots of photon energy dependence of (a) SELF and (b) VELF for  $Se_{80}Te_{20-x}Ge_x$  ( $x = 5, 7$  and  $10$ ) film compositions

The increase of  $E_g$  as well as  $\chi$  with the increase of  $Ge$  content has been rendered on the part of adulterating effect.  $Te$  has an inclination to cause defects states and produce chemical altering in the system, and this causes a compositional alteration in the material due to variation in bond length. So by decreasing  $Te$  the chemical disordering of the system under study decrease and this causes the decrease of lone-pair as seen in Table 2.

### 3.4. Dielectric properties and optoelectronic parameters

The real ( $\epsilon_1$ ) and imaginary ( $\epsilon_2$ ) portions of dielectric constant give information for determining several optoelectrical parameters. These constants have been determined using the equations [43];  $\epsilon_1 = n^2 - k^2$  and  $\epsilon_2 = 2nk$ . The amount of energy loss by electrons while moving through the material and on its surface is known as the volume (VELF) & surface (SELF) energy loss function respectively. Both the VELF & SELF depend on the real and imaginary parts of the dielectric constants through the following relations given in [2,43];  $VELF = \epsilon_2^2 / (\epsilon_1^2 - \epsilon_2^2)$  and  $SELF = \epsilon_2^2 / ((\epsilon_1 + 1)^2 + \epsilon_2^2)$ . Fig. 9 shows the variation of VELF and SELF as a function of  $h\nu$  for  $Se_{80}Te_{20-x}Ge_x$  ( $x = 5, 7$  and  $10$ ) thin films. The two curves have similar nature; however VELF values are larger than SELF values.

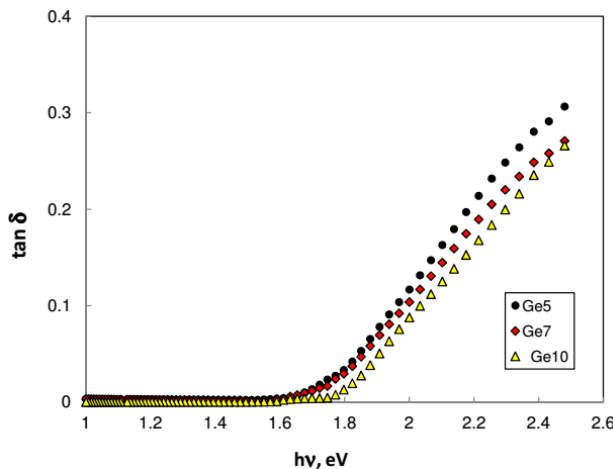


Fig. 10. Plots of photon energy dependence of (a) SELF and (b) VELF for  $Se_{80}Te_{20-x}Ge_x$  ( $x = 5, 7$  and  $10$ ) film compositions

The dielectric loss tangent ( $\tan \delta$ ) is a measure of loss rate in any dissipative system.  $\tan \delta$  is dependent on the real and imaginary parts of the dielectric constant as  $\tan \delta = \epsilon_2 / \epsilon_1$  [44]. The dependence of  $\tan \delta$  on photon energy ( $h\nu$ ) for  $Se_{80}Te_{20-x}Ge_x$  ( $x = 5, 7$  and  $10$ ) thin films has been presented in Fig. 10.

### 4. Conclusion

The optical transmission of  $Se_{80}Te_{20-x}Ge_x$  ( $x = 5, 7$  and  $10$ ) amorphous thin films has been measured in the wavelength range from 500 nm to 2500 nm. An increase in the optical energy gap with increasing the  $Ge$  content has been observed. It has also been found that the refractive index and the absorption coefficient decrease with increasing the  $Ge$  content and as well as with increasing the wavelength. The values of  $N_c$  increase while the value of  $L$  decrease with the increasing of  $Ge$  content. But, the presence of lone pair electron in the system (which well

above the criteria) creates chemical disordering. The stoichiometry  $R$  decreases with the increase of  $Ge$  content. The increase of the above mentioned parameters has been explained on the part of adulterating effect caused by the change in the compositions due to variation in bond formation that disturbs the order of the glass. Adding  $Ge$  to  $Se$ — $Te$  leads to structural changes with the formation of bonds having higher bond energy (*i.e.*  $Ge$ — $Se$  bond energy (2.12 eV) is greater than  $Se$ — $Te$  bond energy 1.76 eV).

### References

- [1] P. Sharma, N. Sharma, S. Sharda, S. C. Katyal, V. Sharma, Progress in Solid State Chemistry **44**, 131 (2016).
- [2] P. Sharma, M. S. El-Bana, S. S. Fouad, V. Sharma, J. Alloys and Compounds **667**, 264 (2016).
- [3] A. K. Singh, Opto-Electronics Review, **20**, 226 (2012).
- [4] M. S. El-Bana, R. Bohdan, S. S. Fouad, J. Alloys and Compounds **686**, 115 (2016).
- [5] S. Guerin, B. E. Hayden, D. Hewak, C. Vian, ACS Combinatorial Science **19**, 478 (2017).
- [6] J. Tominaga, Y. Saito, K. Mitrofanov, N. Inoue, P. Fons, A. V. Kolobov, H. Nakamura, N. Miyata, Advanced Functional Materials **27**, 1702243 (2017).
- [7] S. S. Fouad, Physica B **293**, 276 (2001).
- [8] I. Sharma, A. Z. Khan, J. Optoelectronic. Adv. M. **19**(11-12), 778 (2017).
- [9] S. S. Fouad, S. A. Faek, S. M. El-Sayed, Vacuum **53**, 415 (1999).
- [10] S. S. Fouad, H. M. Talaat, S. M. Youssef, A. El-Korashy, M. M. El-Oker, Physica Status Solidi (b) **187**, k51 (1995).
- [11] P. Sharma, S. C. Katyal, J. Non-Crystalline Solids **354**, 3836 (2008).
- [12] K. A. Aly, J. Non-Crystalline Solids **355**, 1489 (2009).
- [13] F. A. Al-Agel, Materials Science in Semiconductor Processing **18**, 36 (2014).
- [14] M. Mohamed, Materials Research Bulletin **65**, 243 (2015).
- [15] M. Mohamed, S. Moustafa, A. M. Abd-Elnaiem, M. A. Adbel-Rahim, Journal of Alloys and Compounds **647**, 771 (2015).
- [16] N. A. Hegab, M. A. Afifi, H. E. Atyia, A. S. Farid, Journal of Alloys and Compounds **477**, 925 (2009).
- [17] M. A. Afifi, N. A. Hegab, H. E. Atyia, A. S. Farid, Journal of Alloys and Compounds **463**, 10 (2008).
- [18] R. Swanepoel, J. Phys. E: Sci. Instrum. **16**, 1214 (1983).
- [19] R. Swanepoel, J. Phys. E: Sci. Instrum. **17**, 896 (1984).
- [20] B. Derkowska, B. Sahraui, X. Nguyen Phu, G. G. Lowacki, W. Bala, Opt. Mater **15**, 199 (2000).
- [21] R. Naik, R. Ganesh, Thin Solid Films **579**, 95 (2015).
- [22] K. A. Aly, Appl. Phys. A **99**, 913 (2010).
- [23] S. H. Wemple, M. Didomenico Jr, Phys. Rev. B **3**,

- 1338 (1971).
- [24] S. H. Wemple, Phys. Rev. B **7**, 3767 (1973).
- [25] M. N. Amroun, M. Khadraoui, R. Miloua, N. Benramdane, K. Sahraoui, Z. Kebbab, J. Optoelectron. Adv. Mat. **19**(11-12), 771 (2017).
- [26] S. M. Solim, A. Lahmar, H. Zayed, A. M. Salem, G. B. Sakr, N. Teleb, M. El Marssi, Materials Science in Semiconductor Processing **39**, 172 (2015).
- [27] M. Mohamed, M. A. Abdel-Rahim, Materials Science in Semiconductor Processing **27**, 288 (2014).
- [28] P. Sharma, S. C. Katyal, Thin Solid Films **515**, 7966 (2007).
- [29] F. Urbach, Phys. Rev. B **92**, 1324 (1953).
- [30] H. E. Atyia, A. S. Farid, J. Electronic Materials **46**, 357 (2016).
- [31] S. S. Fouad, Vacuum **52**, 505 (1999).
- [32] H. Safak, M. Merdan, O. F. Yuksel, Turk. J. Phys. **26**, 341 (2002).
- [33] H. E. Atyia, N. A. Hegab, Eur. Phys. J. Appl. Phys. **63**, 10301 (2013).
- [34] J. I. Pankove, Optical processes in Semiconductors, Dover Publications, 2010.
- [35] N. Sharma, S. Sharda, V. Sharma, P. Sharma, Chalcogenide Letters **9**, 335 (2012).
- [36] L. Zhenhua, J. Non-Crystalline Solids **127**, 298 (1991).
- [37] D. Lezal, J. Zavadil, M. Prochzka, Optoelectronic. Adv. Mat. **7**, 2281 (2005).
- [38] A. Hruby, Czech, J. Phy. **822**, 1187 (1972).
- [39] S. S. Fouad, M. S. El-Bana, P. Sharma, V. Sharma, Applied Physics A **120**, 137 (2015).
- [40] J. Biceranv, S. R. Ovshinsky, J. Non- Crystalline Solid **74**, 75 (1985).
- [41] J. C. Phillips, M. F. Thorpe, Solid State Comm. **53**, 699 (1985).
- [42] K. J. Rao, Structure chemistry of Glasses, Elsevier Science & Technology, 2002.
- [43] M. S. El-Bana, S. S. Fouad, J. Alloys Compounds **695**, 1532 (2017).
- [44] H. E. Atyia, N. A. Hegab, Optik **127**, 3888 (2016).

\*Corresponding author: pks\_phy@yahoo.co.in;  
pankaj.sharma@juit.ac.in